Synergistic Hybrid-Electric Liquid Natural Gas Drone: S.H.I.E.L.D.

Thierry Sibilli
R&T Thermal Management Specialist
SAFRAN SA
78772 Magny-les-Hameaux, France
FRANCE

thierry.sibilli@safrangroup.com

Sabrina Ayat
Electrical Machines R&T Engineer
SAFRAN SA
78772 Magny-les-Hameaux, France
FRANCE

sabrina.ayat@safrangroup.com

Capucine Senné
Aircraft Energy Systems Engineer
SAFRAN SA
78772 Magny-les-Hameaux, France
FRANCE

capucine.senne@safrangroup.com

Hugo Jouan
Aircraft Energy Systems Engineer
SAFRAN SA
78772 Magny-les-Hameaux, France
FRANCE

hugo.jouan@safrangroup.com

Askin Isikveren
Senior Expert Advanced Aircraft Concepts and Methods
SAFRAN SA
78772 Magny-les-Hameaux, France
AUSTRALIA

askin.isikveren@safrangroup.com

Keywords: *Hybrid Electric, Cryogenic fuel, Liquid Natural Gas, Thermal Management, Unmanned Aerial Vehicle*

ABSTRACT

Issue and Purpose*: With the objective to assess potentially performant hybrid electric architectures, this paper presents an aircraft performance level evaluation, in terms of range and payload, of the synergies between a hybrid electric energy system configuration and a cryogenic fuel system.* ***Scope****: An Unmanned Aerial Vehicle (UAV) is modelled using an aircraft performance tool, modified to take into account the hybrid nature of the system. The fuel and thermal management systems are modelled looking to maximize the synergies effects. The electrical system is defined in series with the thermal engine and the performance, in terms of weight and efficiency, are tracked as a function of the cooling temperature.* ***Results****: The results show up to 46% range increase and up to 7% gain on payload with a reference hybrid electric aircraft that uses conventional drop-in JP-8 fuel. The configuration that privileges a reduction in mass of the electric motors by taking advantage of the cryogenic coolant temperature shows the highest benefits. A sensitivity study is also presented showing the dependency on the modelling capabilities.*

1.0 INTRODUCTION

The quest for enhanced performance military aircraft is continuously raising the bar regarding manoeuvrability, range, endurance, weaponry and surveillance while retaining a low detectability. The energy independence, the economics and the environmental impact are also destabilizing factors that play a role in the optimum solution. In this particular scenario characterized by a set of conflicting requirements, a pondered integrated system design approach is required as a function of the type of flying vehicle and the mission. In the case of an Unmanned Aerial Vehicle (UAV) (Hassanalian, 2017) where quiet operation, reduced heat signature, high electrical load and prolonged operability are of paramount importance, hybrid electric systems have been gathering interest for both the propulsive and the power systems (Hung, 2012; Harmon, 2006). Hybrid-electric conceptual designs show potential fuel savings, reduced environmental impact and introduce new concepts of operation (Pornet, 2015; Brelje, 2019). As stated in previous research (Jansen, 2017), to maximise these benefits a set of technical challenges, like systems integration and thermal management, need to be addressed. The aviation sector, including military applications, seems to be in the midst of a revolutionary era with regards to the electric hybridization, requiring a fully integrated system to gain the most out of these rupture technologies. As by definition, a hybrid-electric system is characterized by an electric power source combined with at least one additional power source. For aeronautic applications, the most common additional power sources are the JP-8 fuel powered gas turbine or the reciprocating engine. In order to improve the performance of these thermal engines, alternative fuels have been considered with the objective to diversify the energy supply, ameliorate the economics and reduce the environmental footprint (Hileman, 2009). Liquefied natural gas (LNG), due to its high specific energy, low price and low CO_2/NO_X/particulate emissions, compared with the JP-8 fuel, stood up as a viable candidate (Withers, 2014). In the last 10 years the price of the LNG has been hovering around a value 60-70%, on a USG basis, lower than jet fuel (EIA, 2019), also showing a 20% reduction on CO_2 and particulate emissions (Withers, 2014). However, other considerations like its storage as a cryogenic liquid, low mass density and thermal management, present technical challenges for aeronautical applications. The hybrid electric configuration seems to be a promising avenue to deliver a more efficient aircraft and the use of LNG, as a non-drop-in fuel for the thermal engine, shows as well a marked potential.

The introduction of electric machines, with their annexed components, will require a revised thermal management and system integration. Additional heat sources and a different set of requirements might undermine the benefits of this architecture. At the same time the LNG has to be stored at cryogenic temperatures (110 K), also requiring a change in phase to be injected into the combustion chamber and is characterized by a considerable high heat capacity. All of this greatly increases its heat sink potential compared to that of the JP-8 fuel. The combination of additional heat sources with a tendency to higher component efficiency or reduced weight and a sound cooling fluid at cryogenic temperatures seems to point towards a synergistic system. Previous research has assessed the potential of hybrid electric energy systems for aeronautic applications (Isikveren, 2019; Pornet, 2015; Brelje, 2019, Jansen, 2017) with some specifically focused on unmanned vehicles (Hung, 2012; Harmon, 2006; Mazur, 2019, Lieh, 2011, Schoemann, Hiserote, 2010, Fredericks, 2013, Eqbal, 2018). Several research projects, starting from the flight of Beech LNG aircraft in 1981 (Flight International, 1981) and the extended NASA evaluation studies (Weber, 1970; Carson, 1980) have weighed the benefits and drawbacks of using the LNG as a replacement or additional fuel. During the recent Boeing Subsonic Ultra Green Aircraft Research (SUGAR) project the LNG was positively assessed as a replacement fuel, showing significant emissions reductions (Bradley, 2012). Recent articles have also underlined the possible benefits, in terms of the thermal management, of having LNG on board of a conventional flying machine (Yin, 2018; Roberts, 2015). A hybrid electric VTOL with an LNG fuelled piston engine and the generator cooled by LNG vapours was recently evaluated (Snyder, 2018; Hartwig, 2018) showing significant benefits compared to an all-electric version of the same VTOL. It is also important to note that cryo-fuels can also be seen as enablers for on-board technology that requires high electrical power instantaneously and/or in a sustained fashion, like High Energy Pulsed Systems (HEPS).

The potential synergies between a cryogenic fuel and the electrical system of a hybrid electric aircraft

seem clear, however, at the present no detailed performance evaluation at aircraft level that includes the fuel, thermal management and electric systems, has been published. The work described here has the objective to show the metrics, in terms of range and payload, of a heavy tactical hybrid electric LNG UAV, named S.H.I.E.L.D as Synergistic HybrId Electric LNG Drone, compared with the same platform but fuelled by JP-8. The paper is organized as follows: the top level requirements and the selected configuration are described in section 2, the hybrid electric energy layout is detailed in section 3, a depiction on the fuel and thermal management systems and their design methods is given in section 4, section 5 is a pleasant read about the sizing methodology, the results are then presented in section 6 and finally in section 7 the conclusions summarize the work done and give the directions for further development.

2.0 HYBRID ELECTRIC AIRCRAFT CONFIGURATIONS: JP-8 AND S.H.I.E.L.D.

The aircraft morphology targeted for this study is a remotely piloted military hybrid electric aircraft, equipped with cameras, sensors, communications equipment and a payload bay. The aircraft can be defined as a Tactical Heavy Combat Medium Altitude Long Endurance UAV, where range and payload are prioritized over endurance, in line with the drone classification presented by Hassanalian (Hassanalian, 2017). The short listed aircraft top level requirements are stated in Table 1-1, notably the cruise Mach number is 0.37 (23000ft), a total payload of 820kg (~1763lbs) and a design range of 800km (~492nm).

Table 2-1: Short Listed Aircraft Top Level Requirements

Flight Profile		Configuration	
Climb	190KCAS / M0.37	Payload	820kg (1763lbs)
Cruise	M0.37	Reserves	Contingence: 2% Block Fuel
Descent	M0.37 / 190KCAS	Wing Loading	200kg/m^2 (4746lb/ft^2)
Design range	800km (492nm)	T/W	0.31
Cruise Alt	23000ft	AR	10

In order to fulfil top level requirements presented in Table 2-1, the selected aircraft configuration was a T-tail mounted twin-motor, for higher reliability, electrical driven fans with a single gas turbine generator and a battery installed in the rear section of the fuselage. In line with the objective of this study of evaluating the synergies between a cryogenic fuel and a hybrid electric energy system, two types of fuels where evaluated: JP-8 and LNG. As a comparison metric, it was decided to keep the same MTOW for both aircrafts with the JP-8 architecture selected as baseline. Figure 2-1 and 2-2 show respectively the JP-8 and the LNG S.H.I.E.L.D. aircrafts. The differences between the two architectures are in the fuel system, the thermal management system and the electrical system. The details of the two arrangements will be described in dedicated paragraphs.

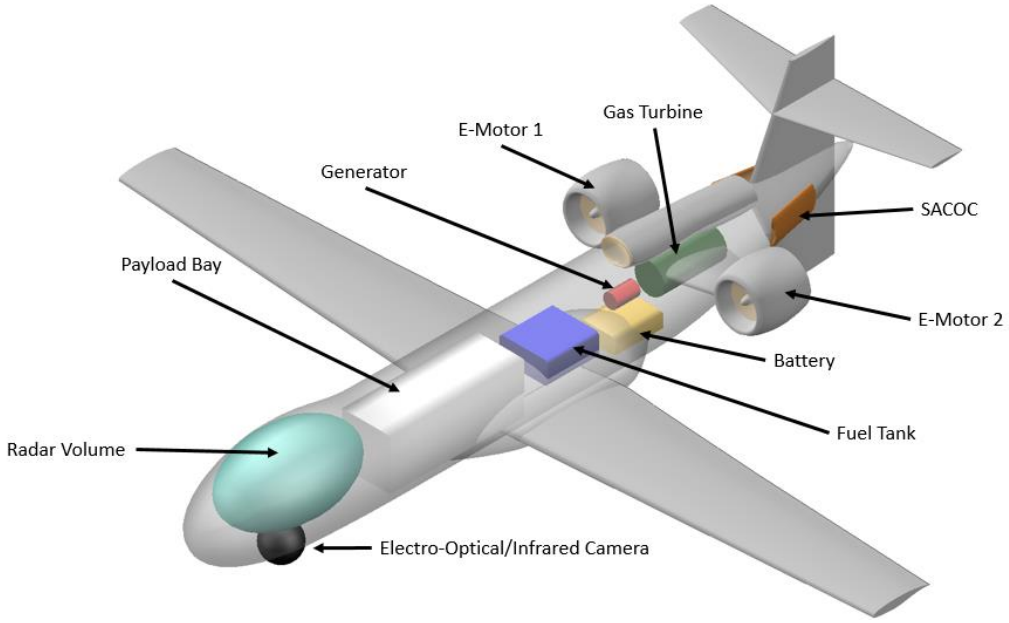

Figure 2-1: JP-8 Aircraft.

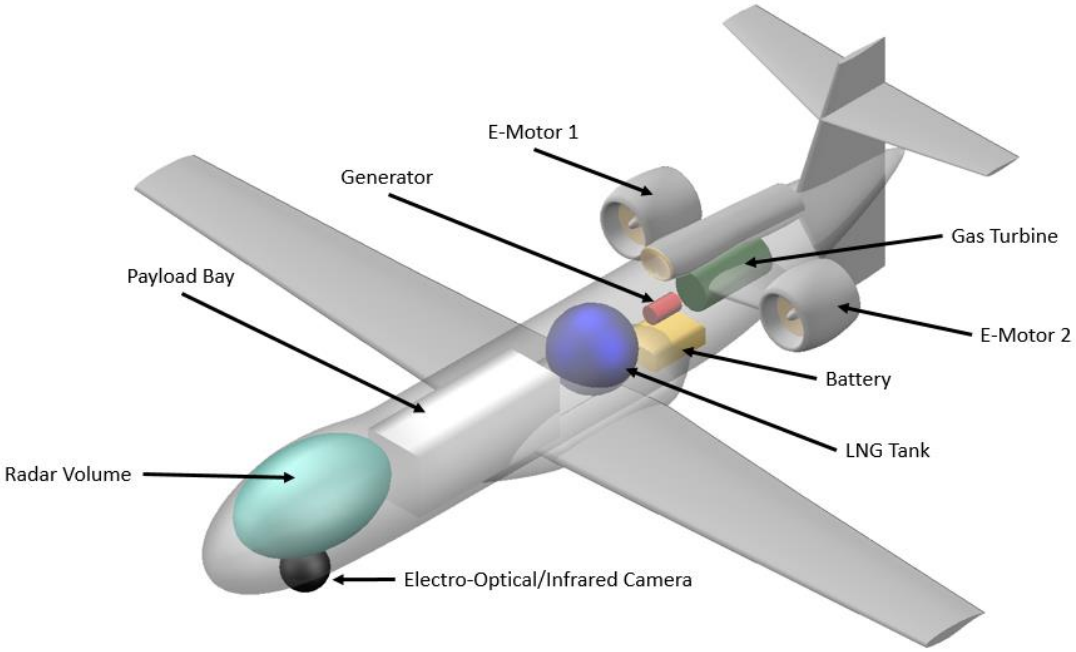

Figure 2-2: LNG Aircraft.

3.0 HYBRID ELECTRIC ENERGY SYSTEM

The hybrid electric configuration selected for both aircrafts was a Series-Full-Turbo-Electric configuration, as shown in figure 3-1. The generator extracts energy from the turbo-shaft, transforming it to electricity, which is then combined in to an electrical node with the energy coming from the battery. To complete the system the controllers and the transformers guarantee the correct functioning and the integration of the

different energy sources. The idea behind the series-hybrid configuration is to operate the gas turbine at an optimum efficiency regardless of the thrust requirements. However, because of the double energy conversion, gas turbine to generator and finally to the motor, the source to sink energy losses can be very large. Given that S.H.I.E.L.D. is characterized by a ducted fan on both sides of the aircraft and only one turbo-shaft, a power gearbox would be necessary in the case of a mechanical drive system. The introduction of an electrical power drive removes the necessity of installing a mechanical drive but adds the weight of the electrical machines themselves, and therefore, requires a minimized weight impact. It is therefore of paramount importance to reduce the various chained electrical losses to minimize the full system conversion losses and to reduce the weight of the full energy system. The energy source for the different flight phases is stated in table 3-1, with a choice between the fully thermal engine, the fully electric and the hybrid configuration. Note that these values were selected arbitrarily for this particular mission and the evaluation of other energy strategies will be the subject of further work. It was also decided not to charge the battery, designed to fulfil the mission requirements shown in table 2-1.

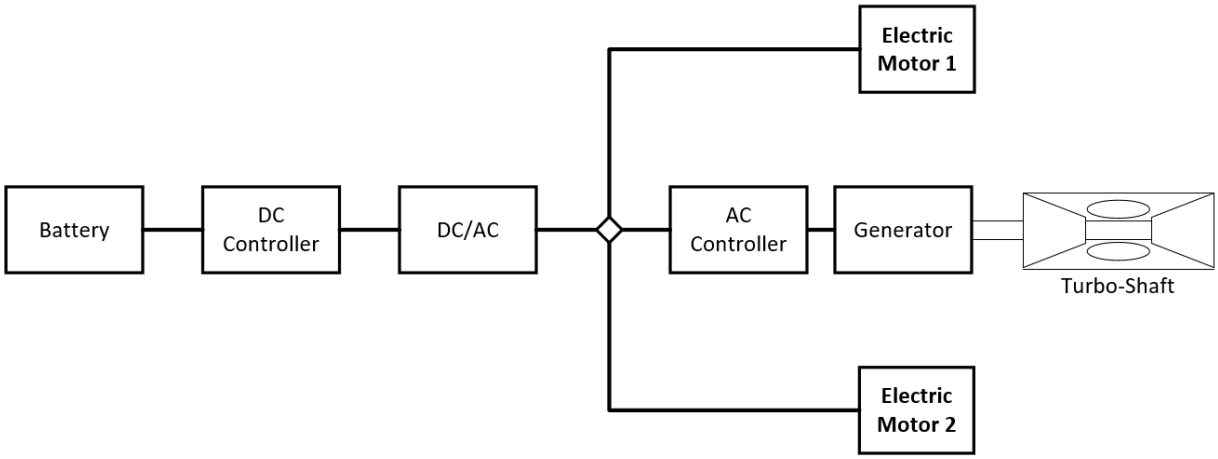

Figure 3-1: Series hybrid electric energy system

3.1 Electric Generator and Motors

A multi-phase radial-flux Permanent Magnet (PM) machine was selected for both the generator and the motors. Basic machine data are provided in Table 3.1-2. Two case scenarios have been considered in this analysis: a first case, where the impact of the temperature on the machine efficiency has been investigated, and a second case, where the impact of the temperature on the machine weight has been explored. For both case scenarios, modelling choices and future investigated are discussed.

Table 3-1: Energy Source for the Different Flight Phases

Flight Phase	Energy Source
TAKEOFF	HYBRID
CLIMB	HYBRID
CRUISE	TE
DESCENT	ELECTRICAL
APPROACH	ELECTRICAL

Table 3.1-2: Basic Machine Data

Rated speed	3000RPM
Rated fundamental frequency	170Hz
Rated output power	250kW (Motor) - 500kW(Generator)
Nominal Mass	49kg/108lbs(Motor) - 98kg/216lbs (Generator)

The machine iron and PM loss components, L_{iron} and L_{PM}, typically decrease with temperature (Chen, 2015; Pyrhonen, 2015; Ruoho, 2010). Therefore, it has been assumed in this study that LNG would be used to cool the windings only. This could be completed for example by circulating a fluid within the winding active length or end-winding assemblies. Similarly, the impact of the temperature on the mechanical loss can be difficult to estimate. Here, due to the assumption that the LNG is only used to cool the windings, the mechanical loss component L_{meca} have been assumed constant for a fixed rotational speed. The contribution of each loss component to the total loss at machine rated speed and at a temperature T_0=120 °C is shown in fig. 3.1-1. Clearly, the copper loss component L_{Cop} due to the DC and AC effects in the stator winding represents the majority of the loss. Here, due to the machine low excitation frequency, the copper loss component due to AC effects represents less than 10% of the total copper loss component.

Therefore, these effects have been ignored. The temperature dependence of L_{Cop} is expressed as follows:

$$L_{Cop}(T) = L_{Cop,T_0}\left(1 + \alpha_{LC}(T - T_0)\right) \quad (1)$$

Where T corresponds to the operating temperature, T0, the initial temperature, $L_{Cop,T0}$ the copper loss component at T_0 and α_{LC}, the temperature coefficient of the copper loss component. For this study copper conductors are used, resulting in $\alpha_{LC}= 3.93\times10^{-3}$/°C. It's important to note that the temperature coefficient, α_{LC}, measured at 293 K is still valid for the range of temperatures considered in this study (Ward, 1971), however, further studies will have to take place to evaluate this assumption.

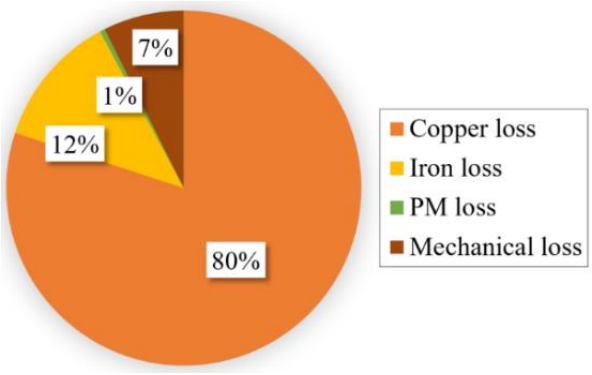

Figure 3.1-1: Loss components for the selected electric machine at its rated operating speed and at T_0=120 °C

The current density in the conductors remained unchanged, and the improved cooling was used to decrease the losses in the conductor, hence improving the machine efficiency. An increase in temperature implies a

rise in resistivity, which leads to an increase in the DC power loss components. However, for the eddy-current related effects, a rise in resistivity implies a decrease in the induced voltage, so a reduction over the AC winding loss arises. This is however valid only for the resistance limited AC effects. The literature suggests that the AC winding loss becomes inductance limited for a high excitation frequency compared to the conductor skin depth (Hanselman, 1995; Wrobel, 2016). For a machine with elevated AC loss, the impact of LNG cooling could therefore be slightly different, and the temperature dependence of AC effects would need to be accounted. Future work is needed to assess these effects. The expression of the efficiency used in this investigation is provided below:

$$\eta(T) = \frac{L_{tot} - L_{cop}(T) - L_{meca} - L_{iron} - L_{PM}}{L_{tot}} \quad (2)$$

The values of each loss component at T_0=373K are listed in Table 3.1-3, where L_{TOT} is the machine total output power.

Table 3.1-3: Loss component at 100°C – Rated Power of 500 kw (Generator)

Loss component	Value [kW]
L_{cop}	7
L_{meca}	0.6
L_{iron}	1.1
L_{PM}	0.1

Finally, a linear expression has been obtained and used in the simulation system:

$$\eta(T) = A_\eta \cdot T + B_\eta \quad (3)$$

Where A_η =-0.0105/°C and B_η = 97.573. An increase of approximately 3% in machine efficiency was predicted when LNG cooling is used, with a winding temperature of around 163K (-110°C).

The other approach involves taking advantage of the improved cooling to reduce the conductor size by increasing the current density in the conductors. By reducing the size of the conductors, the weight of the total machine decreases. A maximum temperature increase ΔT has been calculated dependent upon the LNG and conductor temperature, T, considering a maximum admissible temperature T_{max} = 433K (160°C). The electrical resistance of a single conductor is calculated as:

$$R_\Omega = \frac{R \cdot L}{S} \quad (4)$$

Where ρ is the conductor electrical resistivity, here copper conductors have been used, R=1.68×10^{-8} Ω.m, L and S correspond to the conductor length and cross-section, respectively. The energy dissipated by a conductor for a period, t, can be expressed as follows:

$$E = R_\Omega \cdot I^2 \cdot t \quad (5)$$

Where I is the excitation current within the conductor, here I =100 A for the motors. Finally, the maximum

temperature increase can be expressed as:

$$\Delta T = \frac{E}{m \cdot C_s} \tag{6}$$

Where C_S is the specific heat capacity of the conductor. Here, copper conductors have been used, Cs=385 kJ/kg/°C, and m is the mass of the conductor, defined as follows:

$$m = \rho \cdot L \cdot S \tag{7}$$

Where ρ is the conductor density. Here, copper conductors have been used, ρ=8920 kg/m^3. Finally, the surface of the conductor can be calculated as a function of the previously defined parameters:

$$S = \sqrt{\frac{R \cdot t}{\rho \cdot C_s \cdot \Delta T}} I \tag{8}$$

The mass of the conductor is than calculated from eq. 7, from which the total weight of the windings is derived. The reduction of size of the conductors results on a consequent reduction of size of the stator slots, with therefore a decrease of the total machine weight and size. The same procedure was applied for the generator. Figure 3.1-2 shows mass of electric motor, the generator and the total mass of the electric machines function of the cooling temperature. Point values are also summarized for an LNG cooled machine temperature of 110K (-160°C) and a JP-8/Oil cooled machine temperature of 373K (100°C), including the windings masses. Clearly, the use of LNG can lead to a significant reduction of the machine weight. Further work should be planned to refine the definition of the cooling integration with the machine, increasing the level of confidence of the mass estimation. To summarize, when LNG is used to cool electrical machines, two case scenarios have been considered in this analysis: one where the low temperature results on increased generator and motor efficiencies, and a second case, where the low cooling temperature results in a reduced generator and motor weights. This will result in two different electrical systems, on more efficient and the other lighter that will be evaluated in two different S.H.I.E.L.D. aircraft.

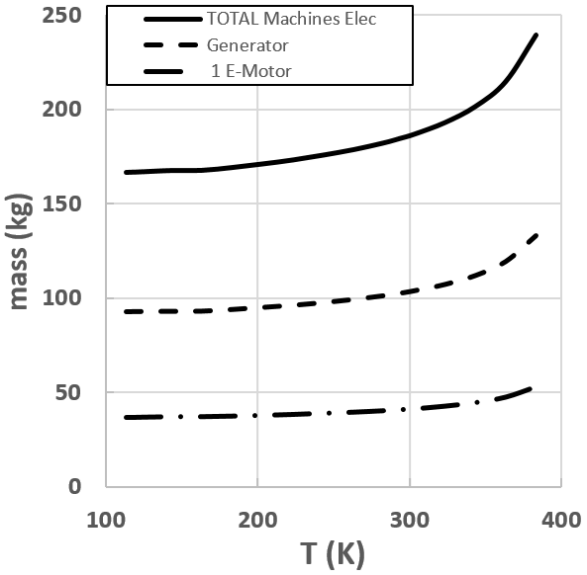

T [K]	$m_{windings}$ [kg]	m_{motor} [kg]	$m_{generator}$ [kg]
110	8.6	27	52
373	20	49	98

Figure 3.1-2: Total, Motor and Generator Electric Machines Masses function of the windings temperature

4.0 FUEL AND THERMAL MANAGEMENT SYSTEMS: JP-8 AND LNG AIRCRAFTS

A schematic overview of the fuel and thermal management systems for both the conventional JP-8 hybrid electric and the LNG hybrid electric aircraft are given respectively in figure 4-1 and 4-2. In both aircraft the fuel acts as the primary heat sink for the cooling of the electrical components. However, for the JP-8 aircraft due to the storage and fuel characteristics an additional heat exchanger, a finned Surface Air Cooler Oil Cooler (SACOC), with a secondary fluid, in this case oil, that rejects the heat to the external air flow, is needed. This has both weight and drag implications, due to the interaction with the air flow. In the case of the LNG aircraft, the fuel storage pressure was set to 1bar (14.5psi), resulting on a 110K (-160°C) storage temperature. This low temperature, the high heat capacity, the change in phase needed before delivering the fuel to the combustion chamber, the higher stability of the natural gas, auto-ignition temperatures 300-350 K higher (Bounaceur, 2016) compared to the JP-8, are all characteristics that result on a radically different scenario compared to an high temperature cooled system. With this basis, the idea behind the fuel system and the thermal management of the LNG aircraft S.H.I.E.L.D. is to maximise the synergies between the cryogenic fuel and the hybrid electric energy system using the cold energy stored into the LNG, at the benefit of the whole aircraft performance. For this particular application it was decided to directly integrate the fuel system with the cooling of the electrical components to increase their efficiency or to reduce their masses, and to install a Nozzle Heat eXchanger (NHX) to reduce the exhaust gas temperature to decrease the Infrared (IR) signature. A counter flow shell and tube heat exchanger was selected in this case.

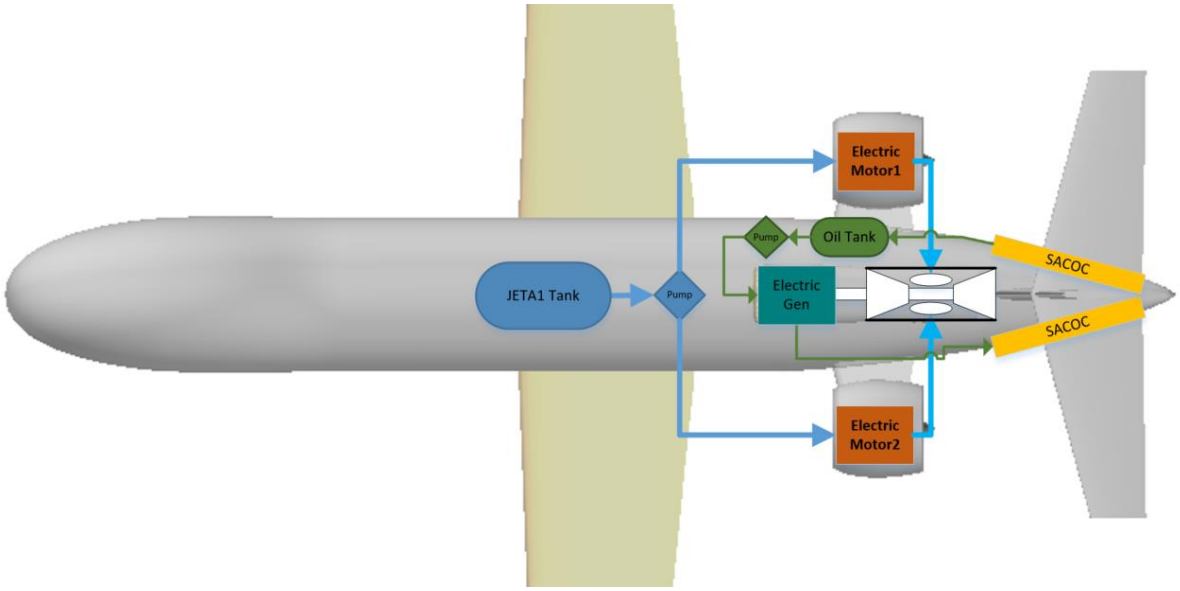

Figure 4-1: Fuel and thermal management systems for the JP-8 aircraft

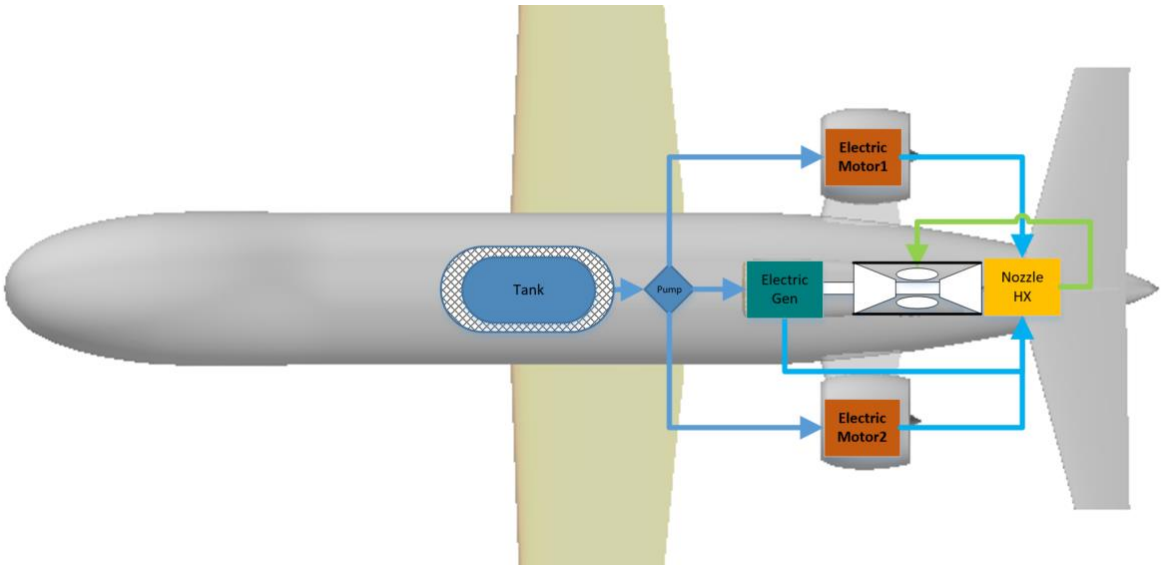

Figure 4-2: Fuel and thermal management systems for the S.H.I.E.L.D. aircraft

4.1 Tank and Distribution Models

Compared with the JP-8 the cryogenic storage temperature requires an insulated tank and part of the distribution system. This is to reduce the boil-off to a minimum and to avoid the formation of ice. A spherical tank shape was selected to minimize the heat entries, lowest surface area volume ratio, and to simplify the structural design. Note that for this particular application there was no need to modify the fuselage section or length to accommodate the less dense LNG, due to the installation of the tank. It was decided to use aluminium for the tank structure and a foam based insulation. To define the thickness of the tank insulation a thermal network model was generated based on the fundamental heat transfer equations. For the fuselage outer flow a flat plate forced convection correlation was selected, listed in eq. 9, 10 and 11 (Cengel, 2015). The external radiation heat transfer was modelled using the small object in a large cavity correlation, as expressed in eq. 12 (Cengel, 2015). For the internal natural convection between the inside walls of the fuselage and the tank, a sphere natural correlation, shown in eq. 13, 14, and 15 (Kaminski, 2005), were deemed as the best choice. The radiation between the internal surface of the fuselage and the external surface of the tank was modelled following the concentric spheres correlation shown in eq. 16 (Cengel, 2015).

$$Q_{FC} = h_{FC} A_{FE} (T_{FE} - T_{FL}) \tag{9}$$

$$h_{FC} = \frac{Nu_L k}{L_{FE}} \tag{10}$$

$$Nu_L = \left(0.037 Re_L^{4/5} - 871\right) Pr^{1/3} \tag{11}$$

$$\dot{Q}_{RE} = \sigma \varepsilon_1 A_{FE} \left(T_{amb}^4 - T_{FE}^4\right) \tag{12}$$

$$k_{eff} = 0.74 k_{air} \left(\frac{Pr}{0.861 + Pr}\right)^{1/4} Ra^{1/4} \tag{13}$$

$$Ra = \frac{g\beta (T_{TE} - T_{FI}) L_{CT}^3}{\alpha \nu} \tag{14}$$

$$L_{CT} = \frac{\left(\frac{1}{r_{TE}} - \frac{1}{r_{FI}}\right)^{4/3}}{2^{1/3}\left(r_{TE}^{-7/5} + r_{FI}^{-7/5}\right)^{5/3}} \tag{15}$$

$$\dot{Q}_{RI} = \frac{\sigma A_{TE}(T_{TE}^4 - T_{FI}^4)}{\frac{1}{\varepsilon_{TE}} + \frac{1-\varepsilon_{FI}}{\varepsilon_{FI}}\left(\frac{r_{TE}}{r_{FI}}\right)^2} \tag{16}$$

The model both the SACOC and the NHX, the lumped parameter e-NTU method (Cengel, 2015) was selected, adding the change in phase for the NHX. For the rest of the components: the pipes and the cooling of the electric machines, a first order heat transfer analysis based on energy balance, was considered sufficient also due to the lack of detailed geometrical design parameters for these parts, necessary for a more comprehensive study. The refinement of the model will be included in the follow-on work. It is important to note that the cooling of the battery, avionics, on-board sensing equipment and the gas turbine oil system, were considered unchanged for both aircraft configurations and therefore not modelled, only taken into account as a mass. In further studies the synergies between the LNG cooling properties and the peculiar UAV thermal loads might result on potentially high further performance improvements. Additionally the foreseen gas turbine efficiency improvements due to higher fuel injection temperature were not included in the all aircraft performance gain. Further work is required to quantify the possible benefits and also evaluate a possible gas turbine efficiency enhancement by coupling the fuel and the gas turbine air cycle itself.

5.0 HYBRID-ELECTRIC AIRCRAFT SIZING METHODOLOGY

The sizing methodology used for this project is an adaptation of the conventional aircraft sizing methods (Mattingly, 2002), based on upon semi-empirical methods, taking into account the novel characteristics of the hybrid electric propulsion system. Figure 5-1 gives a graphical interpretation of the backbone design procedure utilized in this project. Starting from a set of aircraft top level requirements and an aircraft layout, already described in the previous sections, an architecture can be evaluated on the propulsion, systems and airframe levels, via an aircraft disciplines module. The aircraft disciplines module calculates efficiencies, powers, drags and masses for the whole flying vehicle, feeding the thrust table, the energy table and the flight performance module. The adaptation of the method for a hybrid system requires a different definition of the thrust tables, replacing the fuel-flow table with this energy table, therefore introducing the capability of taking into account the dual energy source: fuel and electricity. Additionally the peculiar characteristics of integrating an electrical power system, contributing to the propulsion, add new design parameters that have to be integrated into the whole system of equations.

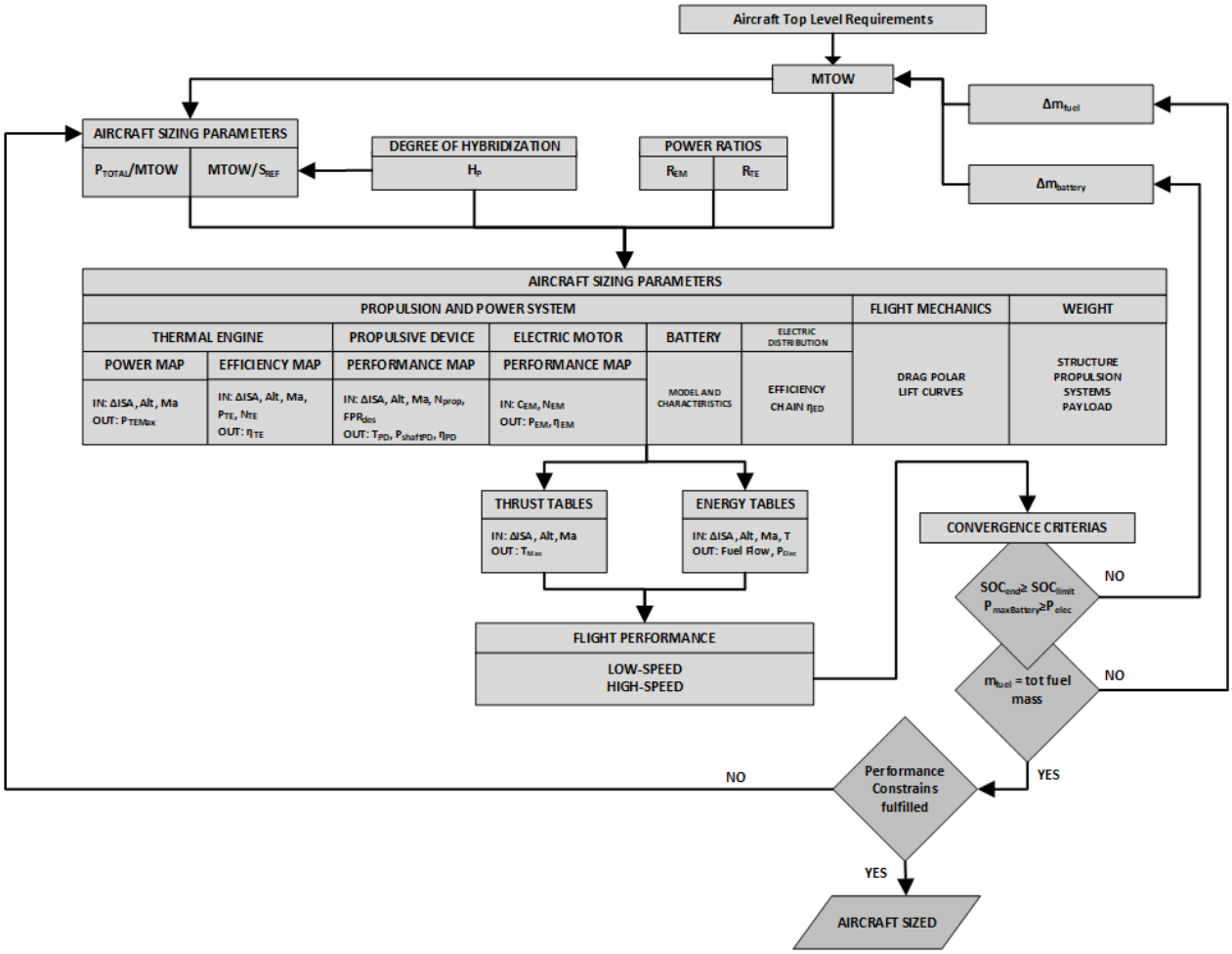

Figure 5-1: Hybrid Aircraft Sizing Procedure

A fundamental parameter is the degree of hybridization for power (H_P) (Isikveren, 2014) that denotes the power sharing between the thermal and electric energy sources, defined as:

$$H_P = \frac{P_{EMMax}}{P_{total}} \tag{17}$$

Where

$$P_{total} = P_{EMMax} + P_{TESLS} \tag{18}$$

The design variables P_{EMMax} and P_{TESLS} are respectively the installed electric motor maximum power and the sea-level static power of the thermal engine. Due to the variation along the mission profile, it is necessary to define power ratings for both the electric motor named R_{EM} as:

$$R_{EM} = \frac{P_{EM}}{P_{EMMax}} \tag{19}$$

And for the thermal engine, named PR_{TE}, as:

$$R_{TE} = \frac{P_{TE}}{P_{TEMax}} \tag{20}$$

Where the P_{TEMax} is a function of the installed sea-level static power P_{TESLS} and the flying conditions (ΔISA, altitude and Mach number). Both P_{TEMax} and P_{TESLS} can be determined using a gas turbine simulation software, e.g. Proosis (EcoSimPro, 2018), or simplified analytical methods. For the work presented here, the commercial software Proosis (EcoSimPro, 2018) was selected generating maps of the gas turbine with ΔISA, altitude, Mach number and the thrust T as inputs and the fuel flow as output. The data were used to generate the thrust and energy tables shown in figure 5-1.

The definition of both tables need to take into account the hybrid electric thermal engine coupling in both energy and thrust terms. In particular the thrust T_{MAX}, output of the thrust tables, is defined as:

$$T_{MAX} = \eta_{PROP} \frac{\left(\eta_{TTE} R_{TE} P_{TEMax} - P_{TEOffTake} + P_{MaxElec}\right)}{V} \tag{21}$$

Where η_{PROP} is the propulsive efficiency, η_{TTE} is the transfer efficiency for the thermal engine, the $P_{TEOffTake}$ is the power offtake from the thermal engine and V is the flight speed. The $P_{MaxElec}$ is defined as the minimum power between the installed electrical motor and the maximum power delivered to the shaft of the electrical motor by the battery, as:

$$P_{MaxElec} = min\left[R_{EM} P_{EMMax};\ \eta_{ES}\left(P_{MaxBattery} - P_{EOffTake}\right)\right] \tag{22}$$

The maximum battery power can be defined as function of the total battery mass, $m_{TOTBattery}$, and the battery gravimetric specific power $\bar{p}$:

$$P_{MaxBattery} = \bar{p} m_{TOTBattery} \tag{23}$$

The electrical power P_{Elec}, output of the energy tables, is defined as:

$$P_{Elec} = \frac{R_{EM} P_{EMMax}}{\eta_{Elec}} \tag{24}$$

Where the η_{Elec} is the combined electric distribution (η_{EDist}) and the motor/generator (η_{EM}) efficiency:

$$\eta_{Elec} = \eta_{EDist} \eta_{EM} \tag{25}$$

The η_{Elec} is function of the selected architecture and the functioning temperature. One of the synergy strategies for S.H.I.E.L.D. is to increase efficiency of the electric machines by operating at low temperature compared to a non-cryogenic cooling. In particular this should lead to an efficiency increase and the aim of this study is to assess the benefits on the full aircraft performance.

The flight performance module will compute the required energy needed to accomplish the mission with inputs from the energy and trust tables, the flight mechanics and the masses. The aircraft is considered sized when a set of criteria, both on the electrical and thermal energy sides, are fulfilled. Note that the masses of the fuel and thermal management systems plus the electrical system will be different between the JP-8 aircraft and the LNG aircraft. It is expected that the fuel and thermal management systems masses will increase for all the LNG configurations while the electrical systems masses will set to lower values

for the LNG configuration targeting a reduced size generator and motors.

6.0 RESULTS

The selected main design parameters and the aircraft layout, obtained applying the procedure previously described are shown in figure 6-1. The parameters and the layout are common for both the JP-8 aircraft and the two S.H.I.E.L.D. aircrafts. As a reminder the difference between the two S.H.I.E.L.D. aircrafts is in the LNG electric synergy strategy, resulting in different efficiency and weight of the generators and motors. The rest of the aircraft, including the hybrid electric energy system, the fuel and the thermal management systems, are the same. The S.H.I.E.L.D. aircraft equipped with lighter electric motors and generator was named S.H.I.E.L.D.1 and the one equipped with more efficient electric motors and generator, S.H.I.E.L.D.2.

Two approaches where selected, variation of range at a fixed payload and variation of payload at a fixed range. For both approaches the aircraft TOW was kept the same as the one defined for the JP-8 aircraft. The TOW, calculated for the JP-8 aircraft is shown in figure 6-1, for two different mission lengths. Note that the intermediate values are linearly dependent.

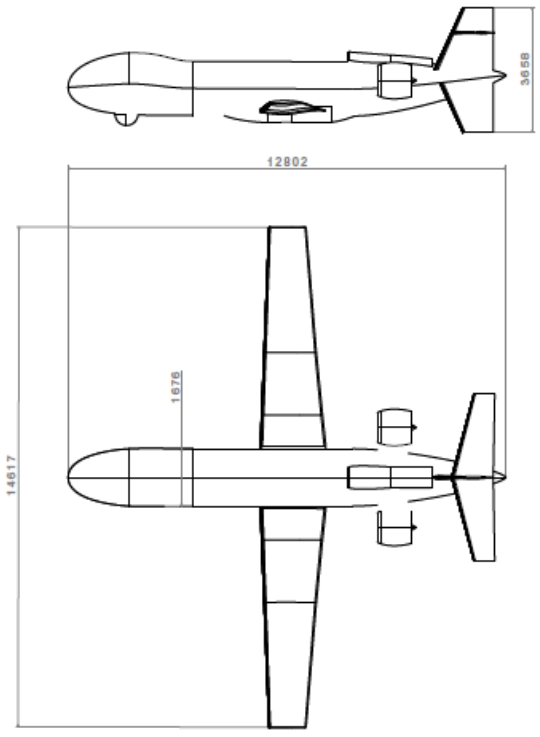

Geometry		Weight	
	22 m²		4600 kg
Wing Area	237 ft²	MTOW	10141 lbs
Aspect ratio	10	MLW/MTOW	>95 %
	1.53 m		
MAC	4.26 ft	MZFW / MTOW	>95 %
Energy Sources		OEW /MTOW	70-75%
	570 kW		1058 Kg
GT SLS Power	746 hp	Max Payload	2332 lbs
Battery System	90 kW		

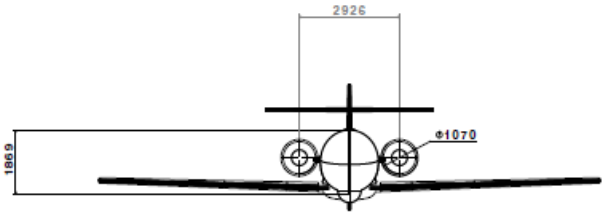

Figure 6-1: Common JP-8 and S.H.I.E.L.D. aircraft layout

Table 6.1: TOW function of Mission Length

	Long	Short
Mission Length	800km/432nm (Design)	300km/162nm
TOW	4600kg/10141lbs	4450kg/9810lbs

Figure 6-2 show the range variations, in terms of percentage, for S.H.I.E.L.D.1 and S.H.I.E.L.D.2 compared to the JP-8 aircraft as a function of mission length, from a 300km (162nm) mission to the design 800km (432nm) mission. For both S.H.I.E.L.D. aircrafts the range variations, compared to the JP-8, are going from +46% at 300km (162nm) to +27% at 800km (432nm) for S.H.I.E.L.D.1, from -3% at 300km (162nm) to 11% at 800km (432nm) for S.H.I.E.L.D.2. The reasons behind these mixed results and the higher performance gains due to the reduction of the mass compared to the increase of efficiency are:

- The gravimetric energy of the LNG is 16% higher compared to the JP-8 (Lemmon, 2018), hence an increase in range for the same mass of fuel burnt;
- For S.H.I.E.L.D.1 due to the synergies between LNG and the cooling of electrical components, a significant reduction of the electric system mass, approximately 30%, allows to carry more fuel;
- For S.H.I.E.L.D.2 due to the synergies between LNG and the cooling of electrical components, the efficiencies of the generator and the two motors increase of about 3%.
- The fuel and thermal management systems for both S.H.I.E.L.D. aircrafts are 11% heavier compared with the JP-8 aircraft.

For S.H.I.E.L.D.1 the reduced mass of the electrical system counter balances the increased fuel and thermal management mass, this leads to an aircraft with increased range for all missions. As the TOW is reduced for shorter missions, the proportion of this extra fuel mass becomes more important resulting in even higher increased range for the S.H.I.E.L.D.1 aircrafts compared to the JP-8. For S.H.I.E.L.D.2 the higher efficiency of the generator and electric motors is not sufficient to counter balance the increased fuel and thermal management mass resulting on a degraded performance for short missions, up to 350 km (189nm), while for longer distances the increased efficiency ensue an improved range overcoming the effects of a heavier aircraft.

It can be appreciated that the assumptions made to define the fuel and thermal management systems might impact the evaluation of its related weight and therefore a sensitivity study was conducted for both the S.H.I.E.L.D. aircrafts. Different levels of uncertainty were defined for the two configurations. In particular a ±40% and a ±15% variation on the fuel and thermal management system weight were applied respectively for the S.H.I.E.L.D.1 and the S.H.I.E.L.D.2 aircraft, at the different mission lengths. The results are shown in figure 6-3 and 6-4 correspondingly for S.H.I.E.L.D.1 and S.H.I.E.L.D.2. It can be seen that for S.H.I.E.L.D.1 the threshold of gain related to the systems weight increases around + 35% for a long mission and 22% for a short mission. For S.H.I.E.L.D.2, the increase of efficiency of the electric machines results on a more modest limit of around +13% for a long mission and -3% for the short mission.

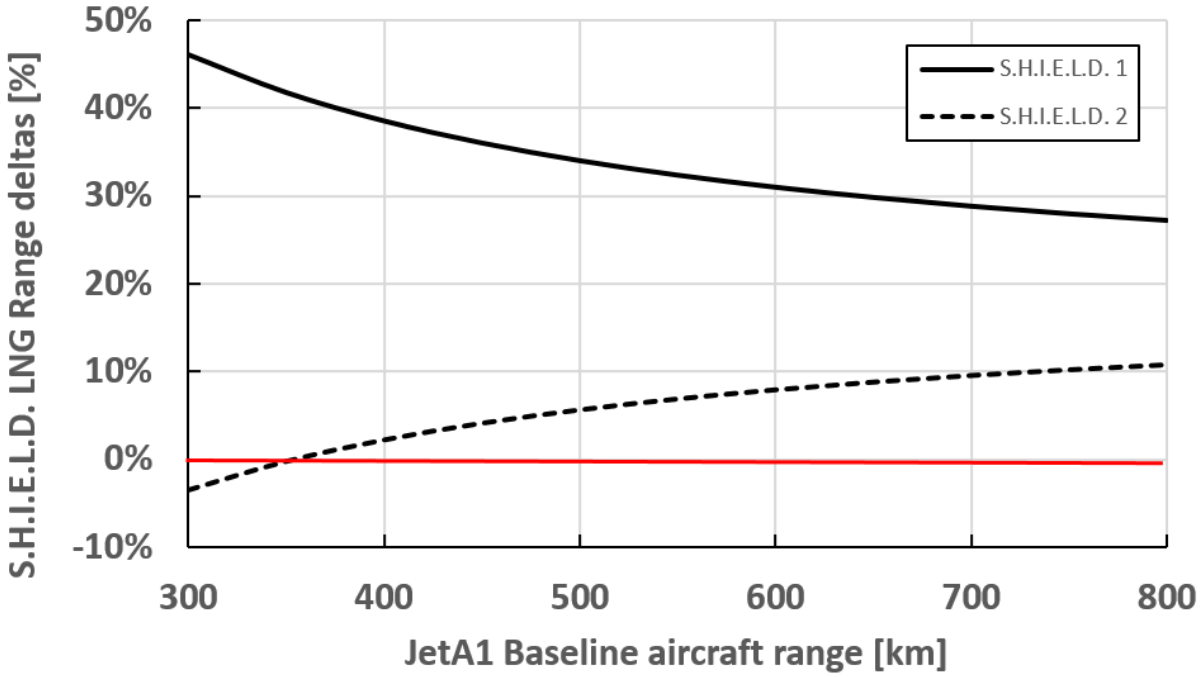

Figure 6-2: S.H.I.E.L.D.1 and 2 range variation compared to the JP-8 aircraft for different mission lengths

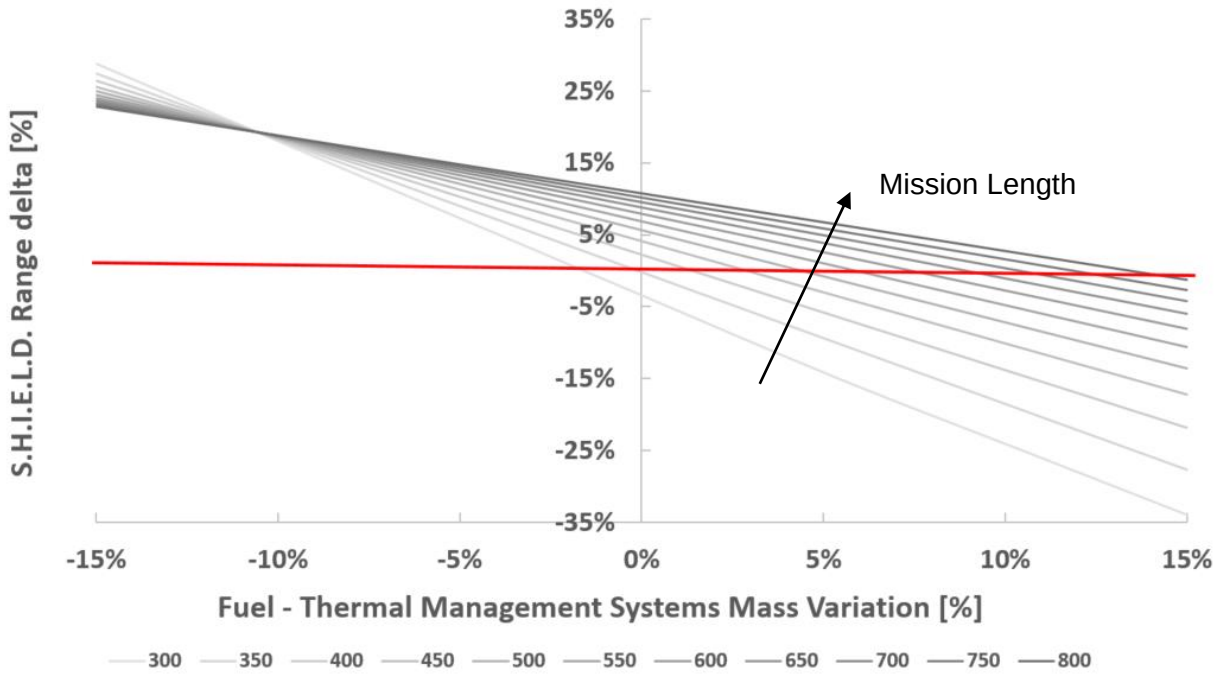

Figure 6-3: S.H.I.E.L.D.1 mass sensitivity study on range variation compared to the JP-8 aircraft for different mission lengths

It is apparent that the reduced weight strategy, S.H.I.E.L.D.1, shows better performance and is therefore less sensitive to mass estimation errors. It is important to remember that these results were obtained with a fixed TOW, only function of the range, and taken from the JP-8 aircraft. Further studies should address the effects of selecting different comparison strategies. Additionally both graphs present a singularity point where all the lines intersect. For both S.H.I.E.L.D. aircraft this is when the weight of the LNG aircraft are the same as the reference JETA1 aircraft. For S.H.I.E.L.D.1 the related range augmentation is due to the 16% higher gravimetric energy of the LNG compared to the JETA1. For the S.H.I.E.L.D.2 this value is higher, being the sum of the 16% higher specific gravimetric energy of the LNG and the 3% electric components efficiency increase.

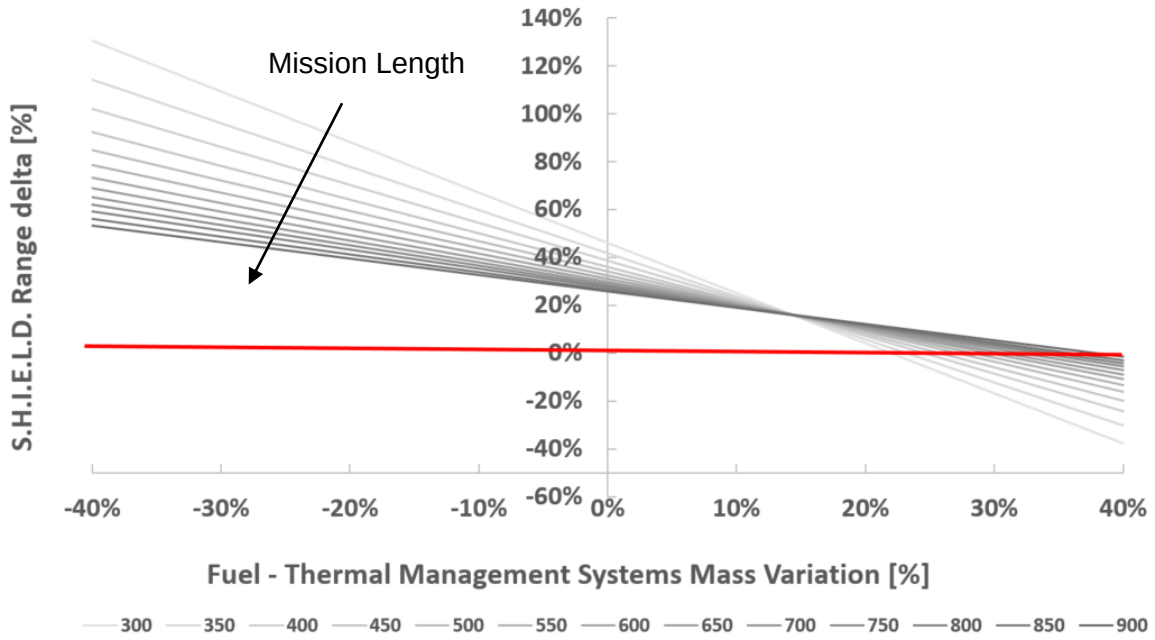

Figure 6-4: S.H.I.E.L.D.2 mass sensitivity study on range variation compared to the JP-8 aircraft for different mission lengths

Another important metric for UAVs is the payload. Its variation was evaluated due to the reduction of weight for S.H.I.E.L.D.1 and the variation of electrical efficiency for S.H.I.E.L.D.2. Figure 6-5 shows the payload trend function of the mission length for both S.H.I.E.L.D. configurations. In accordance with the range plots discussed before the trend is more favourable for the reduced electrical mass strategy of S.H.I.E.L.D.1, with a 7% payload increase compared with the JP-8 aircraft for the 800km (432nm) mission and +5% for the 300km (162nm) mission. In the same way the increased electrical efficiency of S.H.I.E.L.D.2 is not sufficient to support a higher payload for the short 300km (162nm) mission with the same TOW, with a -0.8% reduced payload and a positive value of 2% for the 800 km (432nm) mission. The absolute values are less significant to the fact that additional payload does not contribute directly to the energy differences between the LNG and JP-8 aircraft, moreover the mass of the payload and the fuel are different, with the latter being proportional to the mission length.

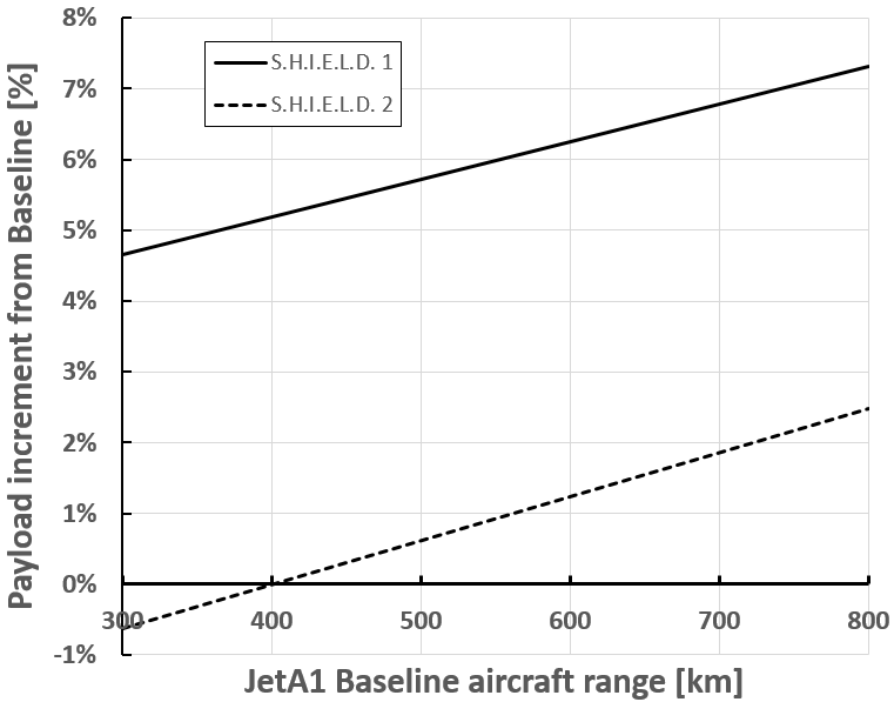

Figure 6-5: S.H.I.E.L.D.1 and 2 payload variation compared to the JP-8 aircraft for different mission lengths

7.0 CONCLUSIONS AND FUTURE WORK

In response to the quest for enhanced performance military aircrafts the work presented here evaluates the performance of a non-conventional Unmanned Aerial Vehicle, where the hybrid electric and the use of alternative non-drop in cryogenic fuels have been combined to explore their synergies and limitations. Starting from the top level aircraft requirements, an LNG and JP-8 aircraft configurations have been defined as a Series-Hybrid-Full-Turbo-Electric, including the electric, fuel and thermal management systems. The synergies have been exploited in terms of increased electrical components efficiency or reduced mass and reduced Infra-Red detectability. The comparison of the two arrangements has shown a marked performance increase in terms of range, especially in the case of a reduced electrical components mass, were the gains are of 46% for a short mission and 27% for the design mission. For the improved electrical efficiency strategy, the LNG shows reduced range, -3%, for a 300km (162nm) mission, and a gain of 11% for an 800km (432nm) mission. The payload study showed less significant absolute values but confirmed the trends, with a maximum 7% payload increase for reduced electrical components mass synergy strategy, for the 800 km (432nm) mission, and a maximum 3% payload increase for the increased electrical components efficiency strategy, for the 800km (432nm) mission. With the configuration and the mission defined for this study, the strategy of using LNG for the thermal management of the electrical machines with the objective of reducing their mass, gives marked performance improvements compared to increasing their efficiency.

A sensitivity study has shown the performance reduction trend for this configuration as a function of the fuel and thermal management systems weight, underlining the importance of minimizing its impact, with a thresholds of 35% weight estimation error for the reduced electrical components mass strategy and 13% for the higher electrical efficiency strategy. In order to better define these boundaries the electric, fuel and thermal management systems models should be improved, not only in terms of single components modelling but also taking into account the installation. The mass gain of the electric components should be

assessed with a critical view on the cooling integration. Future work should address the off-design and transient systems response, as this might considerably change the required configuration.
A refinement of the mass evaluation should also be a priority to increase the validity of the benefit evaluations. The integration of the systems, including the propulsion systems also requires a dedicated study, as this might have a considerable effect on the whole system performance. Other aircraft architectures should be also evaluated, as an example a single electrical powered propulsion. In terms of systems other synergies should be evaluated, including with the main energy source, in this case the gas turbine, and the UAV on board systems, bearing in mind all the effects in terms of both performance and weight. Other hybrid electric configurations should be assessed including an evaluation of different electrical machines and energy sources. Looking at operation and flight techniques, increased range configurations and applications focused on endurance might require a resized fuselage or external tanks to accommodate the LNG fuel tank, due to installation and the lower energy density of the LNG. The augmented drag and weight will have a detrimental effect on the performance of the aircraft, playing a role on the continuous improving equation. The synergies between a hybrid electric energy system and a cryogenic fuel are clear, the related systems have to be defined as an integrated energy system to fully take advantage of them.

REFERENCES

Bounaceur, R., Glaude, P.A., Sirjean, B., Fournet, R., Montagne, P., Vierling, M., Moliere, M., (2016), "Prediction of Auto-Ignition Temperatures and Delays for Gas Turbine Applications", Journal of Engineering for Gas Turbines and Power, 138-2, 021505.

Bradley, M.K., Droney, .C.K., (2012), "Subsonic ultra green aircraft research phase II: N+4 Advanced Aircraft Concept Development", NASA Report CR-2012-217556.

Brelje, B.J., Martins, J.R.R.A, (2019), "Electric, hybrid, and turboelectric fixed-wing aircraft: A review of concepts, models, and design approaches", Progress in Aerospace Sciences, 104, pp. 1-19.

Carson, L.K., Davis, G.W., Versaw, E.F., Cunnington , G.R., Daniels, E.J., (1980), "Study of methane fuel for transport aircraft", NASA Report 159320.

Cengel, Y.A., Ghajar, A.J., (2015), "Heat and mass transfer: fundamentals & applications", 5th edition, McGraw-Hill.

Chen, J., Wang, J., Cheng, D., Wang, Y., Zhu, Y., Liu, Y., (2015), "Modeling of temperature effects on magnetic property of non-oriented silicon steel lamination", IEEE Transactions on Magnetics, 51(11), 1-4.

EcoSimPro (2018). Available online: http://www.ecosimpro.com/ (accessed on 10 December 2018).

EIA (2019), U.S. Energy Information Administration, https://www.eia.gov/, (accessed on 24 March 2019).

Eqbal, S.,A.,M., Fernando, N., Marino, M., Wild, G., (2018), "Hybrid propulsion systems for remotely piloted aircraft systems", Aerospace 2018 5 34, MDPI.

Flight international (1981), "Beech flies with methane", 10 October 1981, p. 1071.

Fredericks, W.J., Moore, M.D., Busan, R.C., (2013), "Benefits of hybrid-electric propulsion to achieve 4x increase in cruise efficiency for a VTOL aircraft", 2013 International Powered Lift Conference.

Hanselman, D.C., Peake, W.H., (1995), "Eddy-currents effects in slot-bound conductors," Proceedings Institute Electrical Engineering - Electrical Power Applications, vol. 142, no. 2, pp. 131–136.

Harmon F.G., Chattot, J. (2006), "Conceptual design and simulation of a small hybrid-electric Unmanned Aerial Vehicle", Journal of Aircraft, 43, September-October 2006, pp. 1490-1499.

Hartwig, J., Niezgoda, B., Kohlman, L., (2018), "A combined thermal-fluid-electrical-mechanical simulink© model for hybrid electric flight vehicle studies", AIAA Aerospace Sciences Meeting 2018, 210059.

Hassanalian, M., Abdelkefi, A (2017), "Classifications, applications, and design challenges of drones: A review", Progress in Aerospace Sciences, 91, pp. 99-131.

Hileman, J.I., Ortiz, D.S., Bartis, J.T. et al., (2009), "Near-term feasibility of alternative jet fuels, final report of PARTNER project 17", Cambridge, MA.

Hung J.Y., Gonzalez, L.F. (2012), "On parallel hybrid-electric propulsion system for unmanned aerial vehicles", Progress in Aerospace Sciences, 51, pp. 1-17.

Hiserote, R.M., Harmon, F.G., (2010), "Analysis of hybrid-electric propulsion system design for small unmanned aircraft systems", 8th Annual International Energy Conversion Engineering Conference, AIAA 2010-6687.

Isikveren, A.T. (2019), "Fundamentals, Pre-Design Methods and Various Studies of Hybrid/Electric Aeronautical Vehicles", Habilitation à Diriger les Recherches thesis, Institut Supérieur de l'Aéronautique et de l'Espace (SUPAERO-ISAE).

Isikveren, A.T., Kaiser, S., Pornet, C., Vratny, P.C., (2014), "Pre-design Strategies and Sizing Techniques for Dual-Energy Aircraft", Aircraft Engineering and Aerospace Technology Journal, Vol. 86- 6, pp.525-542.

Jansen, R.H., Bowman, C., Jankovsky, A., Dyson, R., Felder, J., (2017), "Overview of NASA electrified aircraft propulsion research for large subsonic transports", 53rd AIAA/SAE/ASEE Joint Propulsion Conference.

Kaminski, D. A., Jensen, M. K., (2005), "Introduction to thermal and fluid engineering", 6th edition, Danvers, John Wiley & Sons Inc.

Lemmon, E.W., Bell, I.H., Huber, M.L., McLinden, M.O., (2018) NIST Standard Reference Database 23: Reference Fluid Thermodynamic and Transport Properties-REFPROP, Version 10.0, National Institute of Standards and Technology, Standard Reference Data Program, Gaithersburg

Lieh J., Spahr, E., Behbahani, A., Hoying, J., (2011), "Design of hybrid propulsion systems for unmanned aerial vehicles", 47th AIAA/ASME/SAE/ASEE Joint Propulsion Conference and Exhibit 2011.

Mattingly, J.D., Heiser, W.H., Pratt, D.T., (2002), "Aircraft Engine Design", 2nd edition, AIAA Education Series.

Mazur, A.M., Domansku, R., (2019), "Hybrid energy systems in unmanned aerial vehicles", Aircraft Engineering and Aerospace Technology, 91 (5), pp. 736-746.

Pornet, C., Isikveren, A.T. (2015), "Conceptual design of hybrid-electric transport aircraft", Progress in Aerospace Sciences, 79, pp. 114-135.

Pyrhonen, J., Ruoho, S., Nerg, J., Paju, M., Tuominen, S., Kankaanpaa, H., Stern, R., Boglietti, A., Uzhegov, N., "Hysteresis losses in sintered NdFeB permanent magnets in rotating electrical machines", (2015), IEEE Trans. Ind. Electron., vol. 62, no. 2, pp. 857-865.

Roberts, R.A., Nuzum, S.R., Wolff, M., (2015), "Liquefied natural gas as the next aviation fuel", 13th International Energy Conversion Engineering Conference, AIAA.

Ruoho, S., Haavisto, M., Takala, E., Santa-Nokki, T., Paju, M., (2010), "Temperature dependence of resistivity of sintered rare-earth permanent-magnet materials", IEEE Transactions on Magnetics, vol. 46, no. 1, pp. 15-20.

Schoemann, J., Hornung, M., (2012), "Modeling of hybrid-electric propulsion systems for small unmanned aerial vehicles", 12th AIAA Aviation Technology, Integration and Operations (ATIO) Conference and 14th AIAA/ISSMO Multidisciplinary Analysis and Optimization Conference.

Snyder, C.A., Kohlman, L.W., (2018), "Using liquid natural gas fuel to cryogenically cool and enhance a hybrid electric aircraft power system", Annual Forum Proceedings AHS International, Phoenix USA.

Ward, M.R., (1971), "Electrical engineering science", pp. 36–40, McGraw-Hill.

Yin, F., Gangoli Rao, A., Bhat, A., Chen, M., (2018), "Performance assessment of a multi-fuel hybrid engine for future aircraft", Aerospace Science and Technology, 77, pp. 217-227.

Weber, R. (1970), "Research in USA on LNG as an airplane fuel", Technical Paper NASA TM X-52821, 1970 International Conference on Liquefied Gas, International Gas Union.

Withers, M.R., Malina, R., Gilmore, C.K., Gibbs, J.M., Trigg, C., Wolfe, P.J., Trivedi, P., Barrett, S.R.H., (2014), "Economic and environmental assessment of liquefied natural gas as a supplemental aircraft fuel", Progress in Aerospace Sciences, 66, pp. 17-36.

Wrobel, R., Simpson, N., (2016), "Winding loss separation in thermal analysis of electromagnetic devices", International Conference in Electrical Machines - ICEM16, pp. 2218–2223.

NOMENCLATURE AND CONSTANTS

Symbols

A_η	Electrical Machine Efficiency Coefficient 1 [1/°C]
B_η	Electrical Machine Efficiency Coefficient 2
C	Torque [Nm]
C_S	Conductor Specific Heat Capacity [kJ/KgK]
E	Dissipated Energy [kW]
g	Gravity acceleration [m/s^2]
h	Heat transfer coefficient [W/m^{2}K]
H_P	Hybridization ratio for power
I	Current [A]
k	Thermal conductivity [W/mK]
L	Losses [kW] or Length [m]
M	Mach number
m	Mass [kg]
N	Rotational speed [rpm]
Nu	Nusselt number
P	Power [kW]
$\bar{p}$	Battery specific power [kW/kg]
Pr	Prandtl number
Q	Heat flow [kW]
r	Radius [m]
R	resistivity [Ωm]
Ra	Rayleigh number
Re	Reynolds number
R_Ω	Electrical Resistance [Ω]
S	Section Area [m^2]
T	Temperature [K]
t	Time [s]
α	Thermal diffusivity [m^2/s]
α_{LC}	Conductor loss coefficient [1/°C]
β	Coefficient of volumetric expansion [1/K]
ε	Emissivity [W/m^2]
η	Efficiency
v	Kinematic viscosity [m^2/s]
ρ	Density [kg/m^2]
σ	Stefan-Boltzmann constant 5.67x10^{-8} W/m^{2}K$^-$

Subscripts

Amb	Ambient
Air	Air
Cop	Copper
CT	Convective Tank
EDist	Electrical Distribution
eff	Effective
Elec	Electrical
EM	Electric Motor
EMMax	Electric Motor Max
FE	Fuselage External
FI	Fuselage Internal
FL	Fluid
L	Respective to the length L
LC	Loss Component
Max	Maximum
MaxElec	Maximum Electrical
MaxBattery	Maximum Battery
Meca	Mechanic
PM	Permanent Magnet
PROP	Propulsive
RE	Radiation External
REF	Reference
TE	Tank External or Thermal Engine
TEMax	Thermal Engine Max
TEOfftake	Thermal Engine Offtake
TESLS	Thermal Engine Static Sea-level
TO	Reference Temperature
TOT	Total
TotBattery	Total Battery
TTE	Thermal Engine Transfer Efficiency
FC	Forced Convection

Acronyms and abbreviations

AC	Alternate Current
AR	Aspect Ratio
CAS	Calibrated Air Speed [knot]
CAS	Calibrated Air Speed
DC	Direct Current
GT	Gas Turbine
HTP	Horizontal Tail Plane
ISA	International Standard Atmosphere
LNG	Liquefied Natural Gas
MAC	Mean Aerodynamic Cord [m]
MLW	Maximum Landing Weight [kg]
MTOW	Max Take-off Weight [kg]
MZFW	Maximum Zero Fuel Weight [kg]
NHX	Nozzle Heat Exchanger
OEW	Operating Empty Weight [kg]
PM	Permanent Magnet
PR	Power Ratio
SACOC	Surface Air Cooler Oil Cooler
SHIELD	Synergistic Hybrid Electric LNG Drone
SUGAR	Subsonic Ultra Green Aircraft
T/W	Thrust to Weight Ratio
TOW	Take-off Weight [kg]
UAV	Unmanned Aerial Vehicle
VC	Volume Coefficient
VTOL	Vertical Take-off Landing
VTP	Vertical Tail Plane